

Research Article

Theoretical Simulation and Experimental Investigation of a Rail Damper to Minimize Short-Pitch Rail Corrugation

Caiyou Zhao,^{1,2} Ping Wang,^{1,2} Xi Sheng,^{1,2} and Duo Meng^{1,2}

¹Key Laboratory of High-Speed Railway Engineering, Ministry of Education, Southwest Jiaotong University, Chengdu 610031, China

²School of Civil Engineering, Southwest Jiaotong University, Chengdu 610031, China

Correspondence should be addressed to Ping Wang; 381657901@qq.com

Received 24 August 2016; Revised 7 December 2016; Accepted 27 December 2016; Published 11 April 2017

Academic Editor: Zhike Peng

Copyright © 2017 Caiyou Zhao et al. This is an open access article distributed under the Creative Commons Attribution License, which permits unrestricted use, distribution, and reproduction in any medium, provided the original work is properly cited.

The Cologne-egg fastening systems applied in metro lines, which can be subjected to rail corrugation, are considered in this paper. To understand the mechanism of the formation and development of rail corrugation, dynamic models of the wheel and the track with Cologne-egg fastening system in the frequency domain are developed to analyse the wheel and track vibration behaviour. A field test is also analysed to verify the validity of the mechanism. Using these experimental and theoretical results, the vibration mode of the rail that is responsible for rail corrugation is determined. Based on the results, a novel rail damper that can suppress the track pinned-pinned resonance and smooth the track receptance is presented to minimize short-pitch rail corrugation. It is ultimately found from theoretical simulation and experimental investigation that the application of the rail damper is a long-term and effective method of controlling short-pitch rail corrugation in metro lines.

1. Introduction

With the highly speedy development of China's economy, the process of urbanization has become faster and the traffic demands have increased. Urban rail transit, with the advantages of being large volume, rapid, on time, convenient, safe and environmentally friendly, has become the first choice to solve the traffic congestion of cities. The increase urban mass transit has brought unpleasant environmental vibration and noise problems. To protect the sensitive regions along the rail traffic, such as schools, hospitals, and high-precision laboratories, from vibration, vibration-reducing measures have been applied to subway lines. Using high-elastic vibration damping fastening systems, such as Cologne-egg fastening system, to minimize subway vibration is one of the most popular vibration-reducing measures in China. However, serious railway external and internal noise and vehicle abnormal vibration incidents were observed in some subway lines with Cologne-egg fastening system because the high-elastic vibration damping fastening systems often cause short-pitch rail corrugation, as shown in Figure 1, which aggravates wheel/rail interaction and then increases vehicle and track vibration and noise [1].

Rail corrugation is a very complicated and serious problem in railway engineering. Its initiation and development can magnify the high-frequency wheel-rail contact force, cause a high level of vibration and noise, and accelerate the degradation of the wheel-track system components, shortening their service life. Furthermore, in some cases, rail corrugation can even result in derailment accidents. Therefore, rail corrugation is harmful and should be eliminated [2]. A large number of studies have been carried out in this area, and numerous research documents exist [3]. Based on them, it is clearly apparent that there are many causes that lead to rail corrugation. Nevertheless, rail corrugation continues to be an enigma. According to the corrugation wavelength, rail corrugation can be divided into two categories: long-pitch rail corrugation and short-pitch rail corrugation. Short-pitch rail corrugation usually has a quasi-periodic pattern with wavelengths between 20 mm and 100 mm, and has attracted increasing attention and research since 1980 [4] because it is associated with abnormal vibration, noise nuisance and increased maintenance cost.

From the experimental investigation point of view, Frederick and Bugden investigated and surveyed the problem in

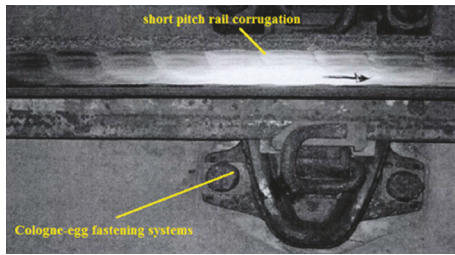


FIGURE 1: State of the rail surface on a track with Cologne-egg fastening system.

detail, including the influence of steel grade, metallurgical structures of corrugations, and type of locomotive, as well as the effects of grinding and initial rail roughness [5]. Moreover, Frederick found that the measured wheel-rail receptances, combined with the creep/force-creep laws and with formulae for rail wear, can be used to predict the initiation and evolution of rail corrugation [6]. In addition, Sato et al. observed that the formation of short-pitch rail corrugation is mainly attributed to the pinned-pinned mode of the track, in which the rail vibrates as if it is pinned at the fastenings [7].

In recent years, the view that rail corrugation is caused by wheel-rail coupling vibrations has been accepted by an increasing number of research scholars. Grassie [8] discovered that rail corrugation at 300–350 Hz and at 750–1000 Hz was associated with the second torsional resonance of the driven wheelsets and the pinned-pinned mode of the track, respectively, when he investigated rail corrugation of North American transit systems. Yan et al. [9] studied the short-pitch rail corrugation with a wavelength of 55 mm that emerged in Beijing metro line 4. It was observed that the short-pitch rail corrugation had a close contact with wheelsets and rail vibration from theoretical simulation and field test investigation, especially at the wheel-rail resonance frequency. Li et al. [10] surveyed the typical short-pitch rail corrugations that appeared in a Chinese metro line. It was found that the inherent characteristics of track structure and vehicle speed had an important influence on the initiation and growth of short-pitch rail corrugation. Furthermore, it was observed that the resonance in a frequency range of 160–300 Hz of the track with vibration dampers is the root cause of the 40–50 mm wavelength short-pitch rail corrugation. Wang et al. [11] investigated the characteristic of short-pitch rail corrugation that appeared in multiple metro lines in China. It was found that the receptance difference at pinned-pinned resonance frequency between the wheel and rail and its periodic variation lead to the periodic variation of wheel-rail interaction state and wheel-rail force. Therefore, the receptance difference and its periodic variation between the wheel and rail are one of the most important factors that results in short-pitch rail corrugation. The most common types of investigated corrugation were classified by Grassie. He summed up the initiation and development mechanisms of rail corrugation three times [8]. In his latest review paper, rail corrugation was classified into six types, and, among them, “pinned-pinned” resonance corrugation was ranked in the first category. Moreover, he determined

that all the documented corrugation types were essentially constant-frequency phenomena. Based on the classification scheme proposed in his latest review paper, the short-pitch rail corrugation of the track with Cologne-egg fastening system investigated in this study belongs to the pinned-pinned resonance corrugation type.

In general, most types of rail corrugation are connected with specific vibration frequencies. Therefore, it is possible to reduce rail corrugation by controlling the wheel-rail interaction and vibration at these frequencies. At present, the principal means are to grind the rails [12]. This could reduce the wheel-rail vibration from the source. However, this requires a significant amount of labour and money and reduces the availability of the networks, and, unfortunately, the corrugation reappears after a period of operation. Theoretically, optimizing the mechanical and geometrical properties of the track structure is another fundamental method to reduce wheel-rail vibration [13–15]. However, the implementation of this method is rather difficult in practice, especially with regard to existing rail lines. Applying lubrication on top of the rail can decrease the wheel-rail interaction, resulting in a reduction of wheel-rail vibration and rail corrugation [16]. However, this will pollute the surface of the track structure. Another solution is the application of rail dampers that are primarily intended to control railway noise and vibration.

Studies on the effects of rail damper/absorber on short-pitch rail corrugation growth began in 2007. Croft et al. [17] made a theoretical analysis of the suppressing effect of rail dampers on wheel-rail forces, wheel-rail vibrations, and rail roughness growth rates. They predicted the rail corrugation growth of the track with rail dampers and found that the peak corrugation level was reduced and shifted to a longer wavelength. Subsequently, in 2011, Wu studied the controlling effects of rail dampers on short-pitch rail corrugation growth [18]. He calculated the evolution process of short-pitch rail corrugation of the track applied with rail absorbers by combining the wheel-track-absorber dynamics and rolling contact mechanics and wear. Furthermore, it was observed that rail absorbers could effectively suppress the short-pitch rail corrugation, whose wavelength is associated with the pinned-pinned resonance. However, there are two points that need to be investigated further. The first is a more realistic model of track and rail damper/absorber. In the abovementioned two studies, the rail was considered as a beam, and the rail damper/absorber was considered as a mass-spring system or beam-spring. In addition, the support length of the fastening system was not taken into account, which had been proven to affect the pinned-pinned resonance of the track [19]. The second is field verification tests. There have been no field tests conducted to demonstrate the theoretical results in the two studies.

To further investigate the validity and applicability of rail absorber/damper in suppressing short-pitch rail corrugation, more thorough research needs to be conducted. Firstly, accurate modelling of the rail and rail damper/absorber should be considered in the theoretical simulation model. Then, parameters that influence track pinned-pinned resonance frequency also should be taken into account. Finally, an appropriate confirmatory experiment should be conducted

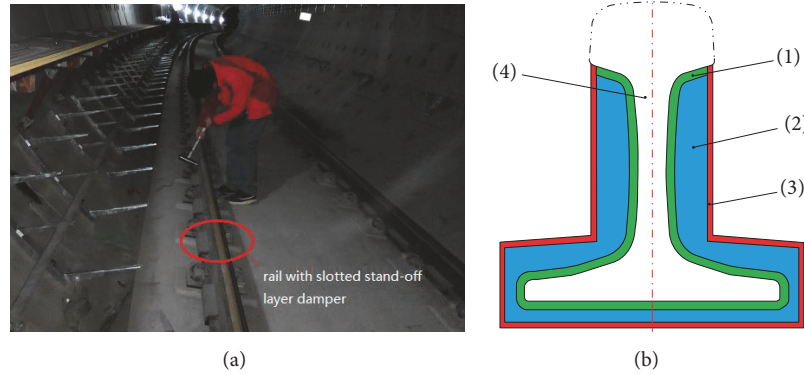


FIGURE 2: Ballastless track with a slotted stand-off layer rail damper and damper cross-section. (1) Slotted stand-off layer; (2) variable-thickness damping layer; (3) constrained layer of uniform thickness; and (4) standard rail.

to verify the theoretical results. In this study, the mechanical properties of a track with a Cologne-egg fastening system, which is used in the Chongqing subway, are analysed, and a novel slotted stand-off layer damper, which has been proven to be an effective measure to control rail vibration and noise [20], as shown in Figure 2, is employed, with the goal of minimizing rail vibrations responsible for short-pitch rail corrugation.

This study was conducted in the following phases. First, investigation and field tests were carried out on the corrugated sections of Chongqing metro line 2. Second, a realistic elastic finite element model of the track with Cologne-egg fastening system in the frequency domain was established, and numerical simulations and wheel and track vibration behaviour analyses were undertaken with this model. Based on the numerical results, an attempt was made to explain the relation between short-pitch rail corrugation and track resonance vibration. Third, the suppressing effect and mechanism of the novel slotted stand-off layer damper on short-pitch rail corrugation are discussed in theory. Finally, in situ observation tests were performed again to verify and evaluate the effect of the rail dampers on minimizing short-pitch rail corrugation.

2. Investigation and Field Test

2.1. Track with Cologne-Egg Fastening System. The track system with a Cologne-egg fastening system used in the Chongqing subway is shown in Figure 3(a). It is composed of the rail, a Cologne-egg fastening system, and track bed slab, as shown in Figure 3(b). The fastening interval is 0.625 m. The track bed slab is connected continuously longitudinally, and its thickness is 0.26 m. The Cologne-egg fastening system is a one-piece, highly resilient rail support consisting of a top plate, a frame, and an elastomer, as depicted in Figures 3(c), 3(d), and 3(e). These first two components are durably vulcanized together via an elastic collar that is made with rubber. This ensures high resistance to slipping and lateral displacement of the rails and thus the most accurate position of the track. In addition, the Cologne-egg fastening system is distinguished from other vibration damping systems by

vibration isolation in all six degrees of freedom. Furthermore, the Cologne-egg fastening system can achieve high insertion loss values due to the low dynamic stiffening of the rubber elastomer.

In the track system, the main load direction is vertical, and the main vibration mode is vertical bending vibration. Thus, the rubber collar of the Cologne-egg fastening system is exposed to compression shear stress. This leads to a linear spring characteristic. This type of compression shear stress is appropriate for the material involved and will guarantee the best mechanical properties of the elastomers and a long life of the rubber-to-metal bond. The rail and top plate are isolated from the track bed slab via a soft rubber elastomer. It can be interpreted as a mass-spring system, the main objective of which is to provide a maintenance-free and silent track.

2.2. First Investigation of the Short-Pitch Rail Corrugation. The selected test site is a curved operational track inside a tunnel with a 500 m radius, where high levels of rail vibrations in both the vertical and lateral directions are excited, and the wheel and rail squeal violently and annoyingly. In situ observation was carried out, and short-pitch rail corrugation was observed, as shown in Figure 4. Consequently, a detailed examination of the mechanism of short-pitch rail corrugation formation in Chongqing metro line 2 was undertaken.

Moreover, in this work, measurements using a tape measure were carried out to clarify the characteristics of the short-pitch rail corrugation of Chongqing metro line 2. It was observed that the wavelength of rail corrugation was 40 mm. The average measured running speed of the test section was 63 km/h. Thus, it can be concluded that the vibration frequency of this section approaches 438 Hz.

3. Analysis of Track Vibration Characteristics in the Frequency Domain

3.1. Definition of Material and Structural Parameters. The model used for the theoretical analysis stemmed from the test site mentioned above and is presented as follows: the rail grid model was constructed of a concrete integrated track bed slab, on which Chinese 60 kg/m rail was fastened with

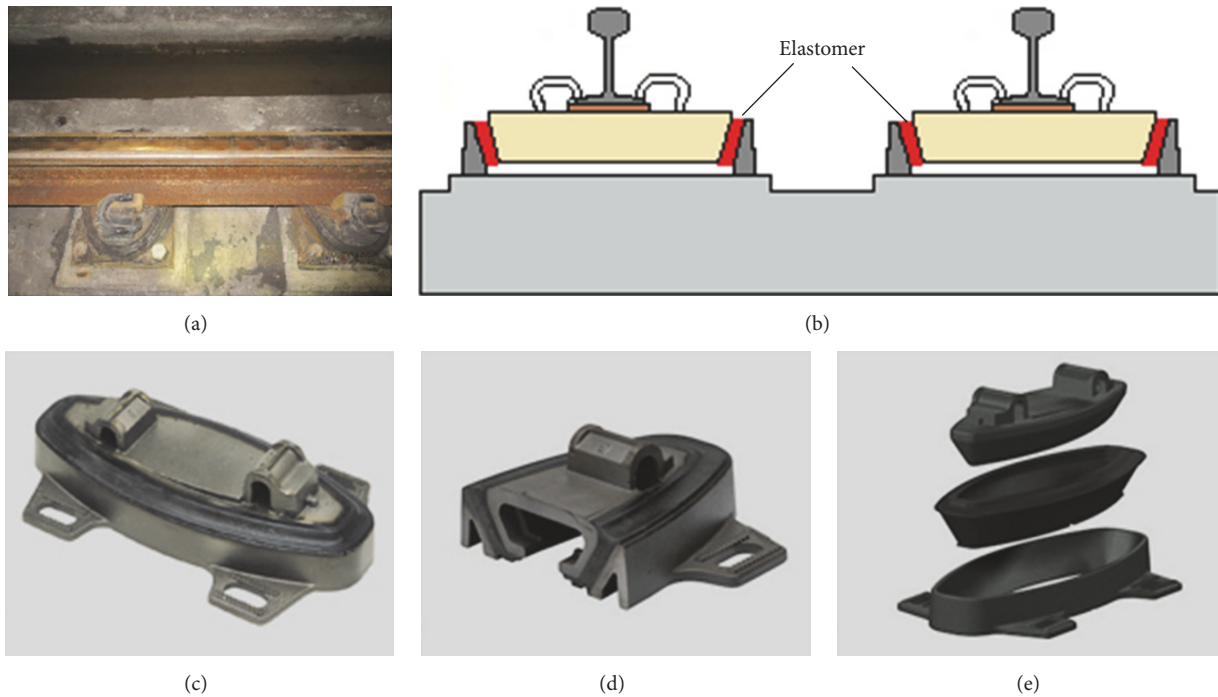


FIGURE 3: Track with Cologne-egg fastening system. (a) Photo of the track with Cologne-egg fastening system; (b) cross-section of the track; (c) photo of the Cologne-egg fastening system; (d) half of the Cologne-egg fastening system; and (e) details of the Cologne-egg fastening system.



FIGURE 4: Short-pitch rail corrugation on Chongqing metro line 2.

a Cologne-egg fastening system. The main parameters of the track structure model are shown in Table 1.

Taking into account the complexity of the model, a finite element method was used to calculate the track vibration characteristic in the frequency domain in different cases. To that end, a three-dimensional track model was developed. The model was 40 sleeper bays long. The numerical experiments indicated that this length was sufficient to study the track vibration characteristic based on the fact that the same results were obtained with a model that was 50 sleeper bays long, as shown in Figure 5.

The rails were modelled using three-dimensional solid elements, and their realistic cross-sectional geometry was

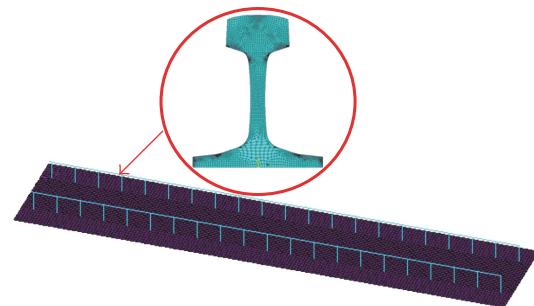


FIGURE 5: Overview of the finite element model and close-ups of the rail.

taken into account. The track bed slab was modelled using an elastic shell element according to realistic geometry. Although the track bed slab was composed of reinforced concrete, a homogeneous isotropic elastic material was assumed here owing to the research results of Gustavson, which showed that linear elastic material properties can be defined for noncracked track concrete components under train passages [21]. The fastening system was represented with two discrete spring and damper pairs consisting of one linear spring and one viscous damper, which were used to simulate the vertical and lateral interactions between the rails and the slabs. The upper nodes of the spring-damper pairs were connected to the rail, and the lower nodes were connected to the slab. In addition, the two ends of rail and the lower track slab nodes were fixed in all three directions. The size of all elements was 0.0039 m.

TABLE I: Main parameters of the track structure model.

Component	Item	Unit	Value
Rail	Per-unit-length mass	$\text{kg}\cdot\text{m}^{-1}$	60
	Young's modulus	MPa	2.06×10^5
	Poisson's ratio	—	0.3
Fastening system	Vertical stiffness	$\text{kN}\cdot\text{mm}^{-1}$	12.07
	Vertical damp	$\text{kN}\cdot\text{s}\cdot\text{mm}^{-1}$	1361.12
	Lateral stiffness	$\text{kN}\cdot\text{mm}^{-1}$	7.58
	Lateral damp	$\text{kN}\cdot\text{s}\cdot\text{mm}^{-1}$	974.27
	Fastening spacing	m	0.625
	Support length	m	0.15
Track bed slab	Young's modulus	MPa	3.35×10^4
	Poisson's ratio	—	0.2
	Thickness	m	0.26

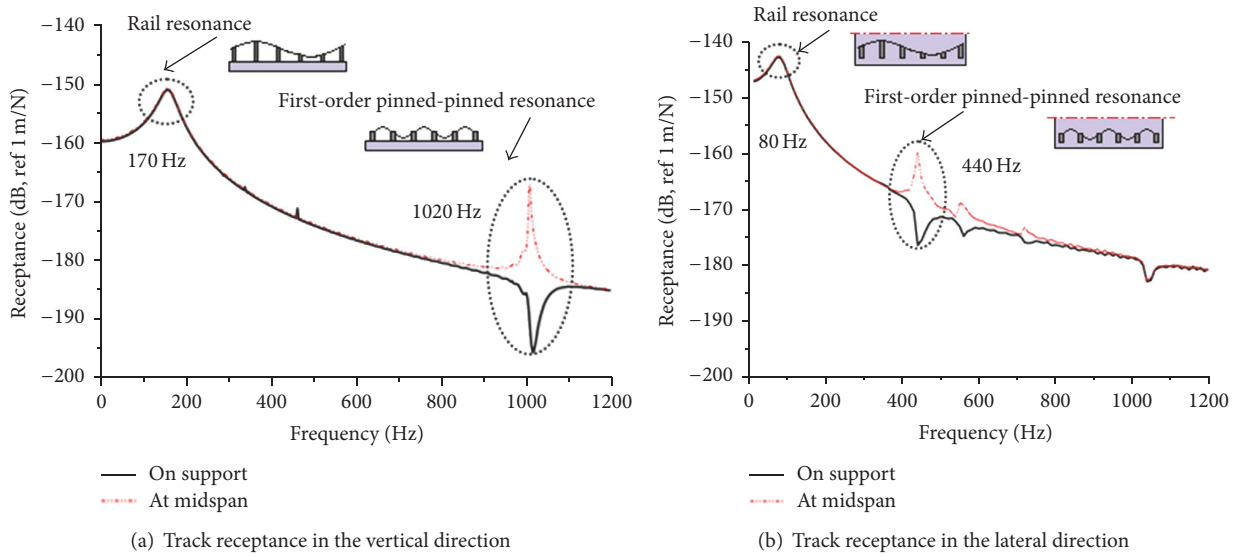


FIGURE 6: Track receptance spectra.

3.2. Dynamic Characteristic of the Track System. Based on the established model, the receptance of the track at the frequency of 0–1200 Hz in the vertical and lateral directions could be calculated. Two reference positions for the typical dynamic track behaviour were investigated. The first is the excitation and vibration recording point on the support, namely, above the fastening system. The other is the excitation and vibration recording point at midspan. Their vertical and lateral receptance spectra, with the corresponding operational deflection shapes obtained in each maximum, are shown in Figures 6(a) and 6(b), respectively.

From Figure 6(a), it is observed that the vertical track receptance spectrum at the frequency range is below 1200 Hz. There are two important frequencies, 170 Hz and 1020 Hz. At 170 Hz, the rail both on support and at midspan vibrates most violently in the vertical direction. Its corresponding mode shape is that rails vibrate vertically on a fastening. At 1020 Hz, the rail receptances in vertical direction at the two positions are diametrically opposed, namely, a crest at midspan and trough on support. Meanwhile, its corresponding mode

shape is a first-order vertical pinned-pinned resonance. The rail nodes on support coincide with the modal node, and the rail nodes at midspan coincide with the node with the largest vibration amplitude, which is why the vertical track receptance spectrum has a characteristic at the frequency of 1020 Hz. Moreover, at the frequency of 1020 Hz, there is a significant gap at the track receptance between the position on support and at midspan.

Figure 6(b) shows the lateral track receptance at the frequency range of 0–1200 Hz. There are also two momentous frequencies, 80 Hz and 440 Hz. At 80 Hz, the lateral rail receptances both at the position above the fastening and at midspan reach the maximum. The corresponding mode shape is that rails vibrate on fastening laterally. The other frequency, 440 Hz, almost coincides with the vibration frequency of the test section with a short-pitch rail corrugation in Chongqing metro line 2. The rail receptances in the lateral direction at the two particular cases are also opposite, that is, a crest at midspan and a trough on support. The modal analysis shows that this frequency corresponds to the first lateral

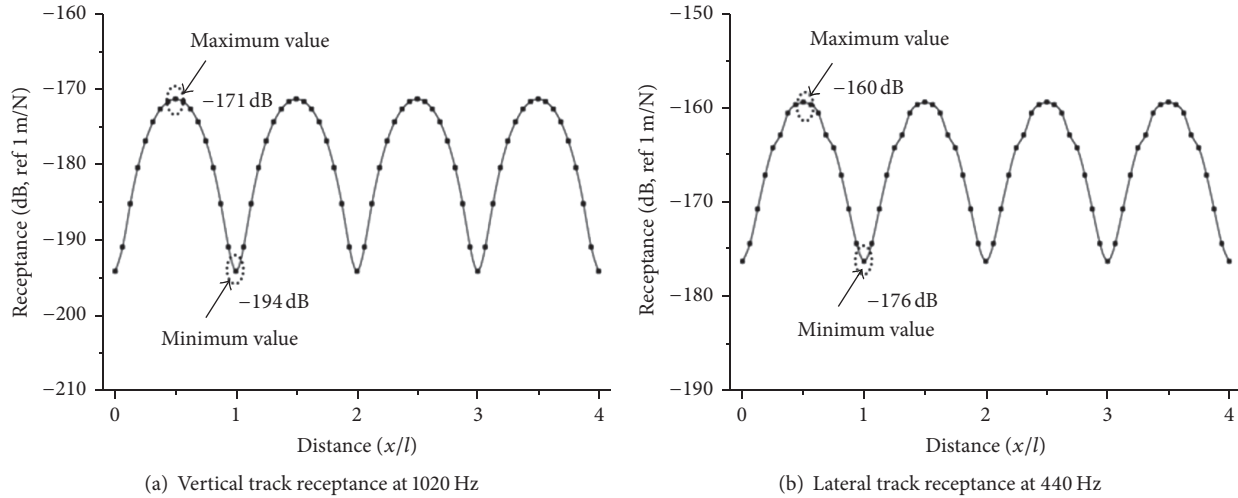


FIGURE 7: Receptance at different positions on the longitudinal beam of track at the first pinned-pinned frequency.

pinned-pinned resonance of the calculated track system. Furthermore, at the frequency of 440 Hz, there is a significant difference in the track receptance between the position on support and at midspan. Namely, the first lateral pinned-pinned resonance is the most likely to cause short-pitch rail corrugation.

In summary, the track receptance on support and at midspan varies considerably at the pinned-pinned resonance frequency due to discontinuous support.

To investigate the distribution of track receptance along the longitudinal direction of the track at the first pinned-pinned resonance frequencies, the track receptance at different positions of four sleeper bays was calculated again. Each sleeper bay is equally divided into sixteen sections and seventeen points to apply a unit vertical harmonic force at a frequency of 1020 Hz and a unit lateral harmonic force at a frequency of 440 Hz. The track receptance at different positions along the longitudinal direction of the rail at these two pinned-pinned frequencies is as shown in Figure 7. It can be observed that there is an obvious periodic difference variance of the track receptance at the pinned-pinned frequency between the positions on support and at midspan. In addition, Figure 7(a) shows that the maximum track receptance is -171 dB, and the minimum track receptance is -194 dB. The difference between the two is up to 23 dB, which means that the vertical track receptances on support and at midspan differ greatly at the first vertical pinned-pinned frequency of 1020 Hz. Figure 7(b) shows that the lateral track receptance varies with different positions along the rail. The maximum track receptance is -160 dB, and the minimum track receptance is -176 dB. The difference between the two is up to 16 dB, which indicates that the lateral track receptances on support and at midspan differ greatly at the first vertical pinned-pinned frequency of 440 Hz. This wide variation of track receptance greatly increases the dynamic instability of the track.

3.3. Variation in Receptance Difference of a Discontinuous Supported Rail-Wheel System. The discontinuous support

of the track system results in modal characteristics and variations in track receptance at different positions along the rail. The vehicle unsprung mass of 800 kg, which is the most typical value of the metro vehicle system in China, was used to calculate the wheel receptance spectrum in this study, as shown in Figure 8. Combining Figures 7 and 8, it can be concluded that there is a crossover point between the track receptance line and the wheel receptance line. The corresponding vertical and lateral frequencies are defined as f_{v0} and f_{l0} , respectively. The track receptance is larger than the wheel receptance above f_0 and is much larger than the wheel receptance at the frequency equal to and above the rail resonance frequency, including the first vertical and lateral pinned-pinned frequency. Therefore, the dynamic displacement of the rail is larger than the wheel under excitation of a similar force, and this displacement difference results in the periodic variation of the wheel-rail contact force.

Considering the structural symmetry and periodicity of the track system, the wheel-track receptance differences along the half sleeper bay track at the first pinned-pinned frequency were calculated, as shown in Figure 9. As depicted in Figure 9(a), the maximum vertical wheel-track receptance difference at different positions along the rail at the pinned-pinned frequency of 1020 Hz is 2.65×10^{-9} m/N at midspan, and the minimum value is 1.39×10^{-9} m/N on support; the difference between them is 1.26×10^{-9} m/N. As demonstrated in Figure 9(b), the maximum lateral wheel-track receptance difference at different positions along the rail at the pinned-pinned frequency of 440 Hz is 1.29×10^{-8} m/N at midspan, and the minimum value is 9.74×10^{-10} m/N on support. The difference between them is 1.1926×10^{-8} m/N.

In conclusion, the lateral wheel-track receptance difference is much greater than the vertical wheel-track receptance difference at the first pinned-pinned frequency. The large lateral wheel-rail receptance difference would lead to severe wheel-rail force and severe rail vibration.

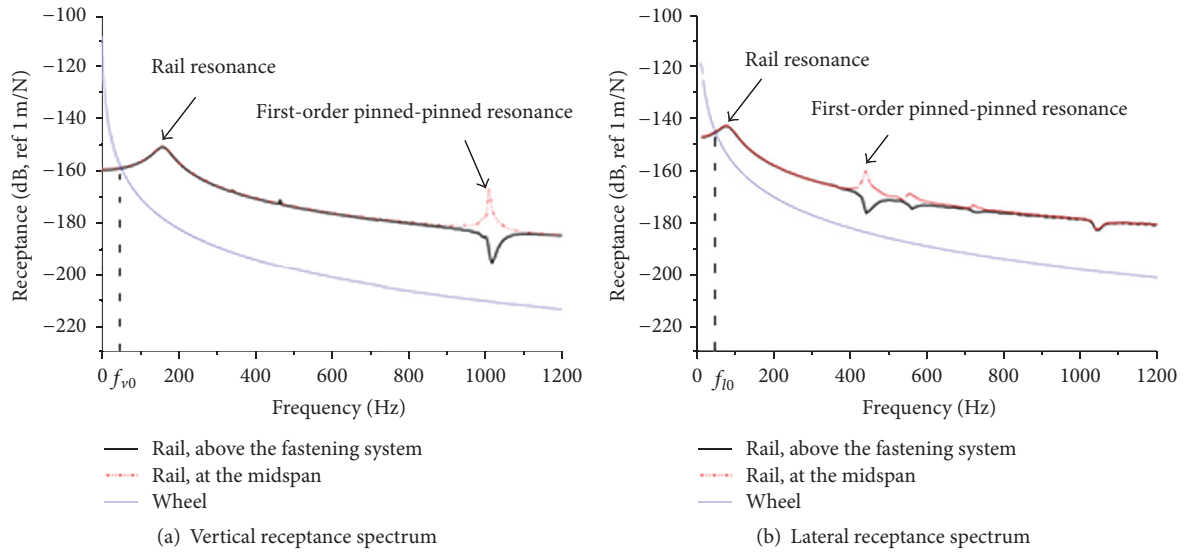


FIGURE 8: Comparison of the wheel and track receptance spectra.

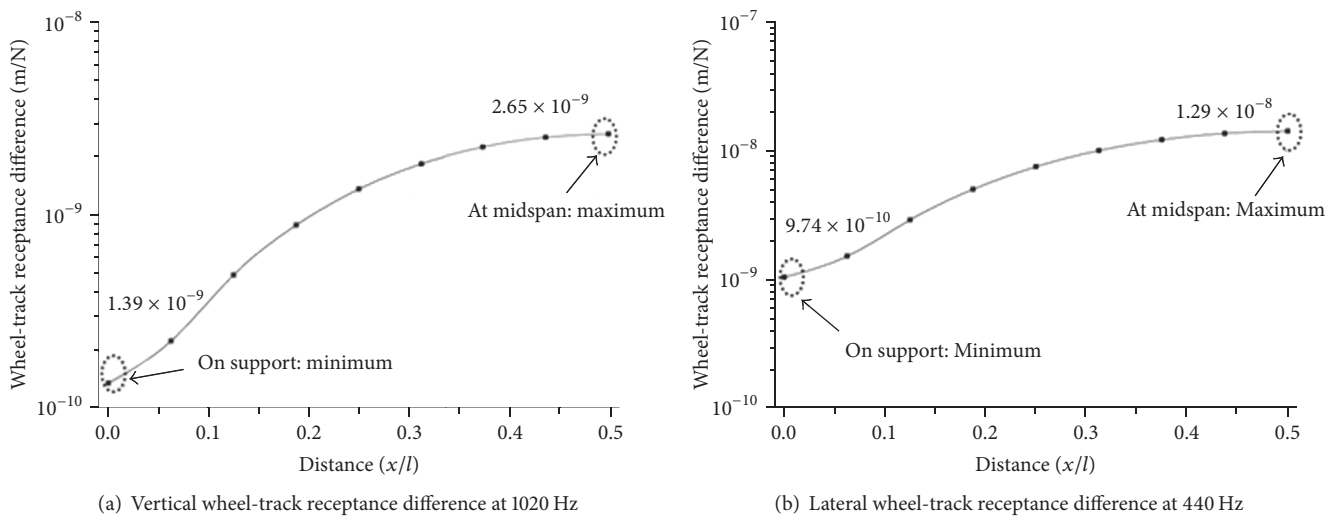


FIGURE 9: Wheel-track receptance difference along the rail at the first pinned-pinned frequency.

3.4. Interpretation of Short-Pitch Rail Corrugation Initiation and Evolution. In general, the initial track roughness irregularity existed in high-speed rail lines and metro rail lines. In combination with the variation in the vertical wheel-track receptance difference, the wheel-rail vertical-longitudinal rolling contact shows unsteady-state dynamic behaviour. The wheel-rail contact force on the interaction face is also an unsteady-state dynamic force while the wheel rolls along the rail, as shown in Figure 10(a). When the moving speed of the wheel exceeds a certain value, the corresponding excited vibration frequency of the track is more than a certain value f_0 (as depicted in Figure 8); especially for the first pinned-pinned frequency, the vertical displacement of the track will be larger than that of the wheel. In addition, it will lead to an unsteady wheel-rail rolling contact model, which is in the form of “contact-separation-colliding-contact.” Short-pitch

rail corrugation will be caused on the vertical wheel-rail interaction surface if the wheel-track receptance difference is large enough at a certain frequency and if the moving speed is constant.

On the other hand, when the wheel rolls along the rail, there is also lateral sliding in the wheel-rail contact surface due to the gradient tread design. Similar to the vertical dynamic behaviour, due to the variation in the lateral wheel-rail receptance difference, the lateral periodic wheel-rail displacement difference will cause lateral sliding friction between the wheel and rail contact surfaces and generate wheel-rail contact surface wearing. Once the moving speed of the wheel is invariable, the combination of the lateral and vertical vibration of the rail will lead to contact force fluctuation and lateral alternating sliding, as shown in Figure 10(b). The wheel-rail receptance difference variations,

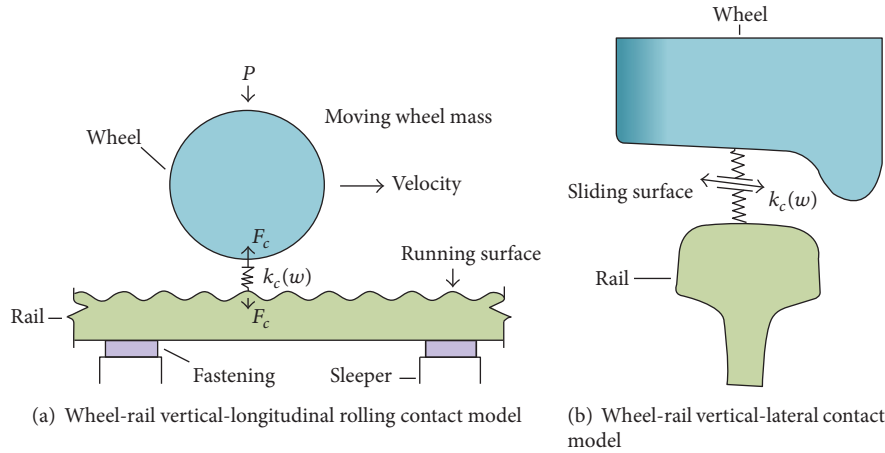


FIGURE 10: Wheel-rail contact model.

in combination with the wheel-rail contact force variation along the longitudinal direction, result in rail surface wear and the formation of a standing wave shape. Because the wheel running tread has a definite width, the basic form of the wheel-rail contact surface is almost an ellipse. The lateral vibrating and sliding wearing trace has a wide band shape similar to the short-pitch rail corrugation that is observed in Chongqing metro line 2.

From the abovementioned analysis, it can be concluded that the short-pitch rail corrugation observed in Chongqing metro line 2 is mainly due to two factors, namely, the fixed moving speed of the wheel and the large wheel-track receptance difference at the first lateral pinned-pinned frequency. In general, the moving speed of a metro vehicle is unchangeable according to the operation scheme. Hence, a decrease in the wheel-track receptance difference is an effective method to minimize the short-pitch rail corrugation.

4. Modelling the Minimizing Effect of Rail Dampers on Short-Pitch Rail Corrugation

4.1. Introduction of a Novel Slotted Stand-Off Layer Damper. Recent research has demonstrated that rail dampers can decrease the dynamic interaction forces and shift the force spectrum to longer wavelengths and therefore reduce noise and roughness growth [17, 18]. Here, a novel slotted stand-off layer damper, developed by the authors and shown in Figure 11, was introduced to investigate the minimizing effect of rail dampers on short-pitch rail corrugation initiation and growth.

In Figure 11, h_{s1} is the zone thickness of the slotted stand-off layer without slots, h_{s2} is the slot thickness of the slotted stand-off layer, t_{s1} is the slot width, t_{s2} is the zone width of the slotted stand-off layer without slots, h_c is the thickness of the constraining layer, $t_{c1} \sim t_{c3}$ are the three important structural sizes of the constraining layer, l_{s1} is the zone length of the rail foot without the slotted stand-off layer, l_{s2} is the zone length of the rail foot with the slotted stand-off layer, and α is the slope of the constraining layer. The values of these parameters are shown in Table 2.

TABLE 2: Configuration of the damper.

Parameter	Value
h_{s1} (mm)	6
t_{c1} (mm)	100
α	4%
t_{c2} (mm)	55
t_{c3} (mm)	45
h_c (mm)	2
h_{s2} (mm)	3
t_{s2} (mm)	20
t_{s1} (mm)	30
l_{s2} (mm)	370
l_{s1} (mm)	135

As depicted in Figure 11, the novel rail damper consists of three major parts: an inverted T-shaped constraining layer of uniform thickness that is connected to a rail with a slotted stand-off layer of uniform thickness that is sandwiched between the slotted stand-off layer and the slotted constraining layer with a thickness-variable damping layer. Each layer was glued together with a strong adhesive. The outermost layer of the clasp, which is made of alloy spring steel, is an extra step to verify the firm bonding between the rail and dampers. The slotted stand-off layer was made from Dyad606, whose density and Young's modulus of elasticity are 1200 kg/m^3 and 500 MPa , respectively. The material used for the constraining layer was steel-3Cr13Mo, with an elastic modulus of $E = 206 \text{ GPa}$. VER-IPN was chosen as the material for the damping layer, and its loss-factor and elastic modulus in the temperature and frequency ranges of interest are given in [20].

The utilization of rail dampers can reduce the wheel-rail interaction forces and change the dynamic response of the rail, shifting the pinned-pinned frequency and smoothing the track receptance, which is very helpful for suppressing the worsening of short-pitch rail corrugation. This advantage can address the "remembering and reappearing" characteristic of

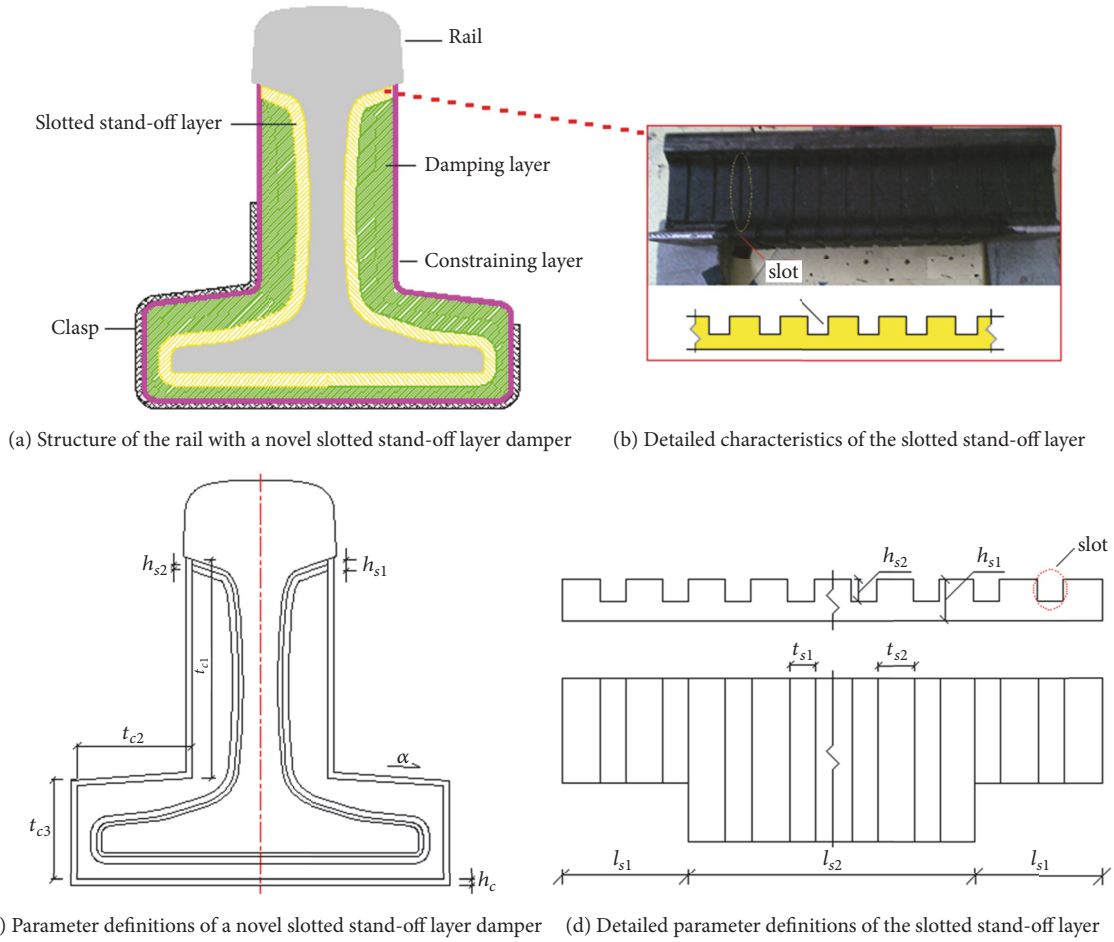


FIGURE 11: Structural composition and parameter definitions of the slotted stand-off layer damping treatment.

rail corrugation. In the next section, a theoretical simulation of the suppressing effect of the rail dampers on short-pitch rail corrugation initiation and growth based on the abovementioned mechanism of the variation in the difference between the wheel and rail receptances was conducted.

4.2. Simulation Method. The model applied for theoretical analysis is the same as the one used in Section 3.1. The rail dampers were also modelled using three-dimensional solid elements, and their realistic geometry was taken into account, as shown in Figure 12. The receptance spectra of the track with dampers are shown in Figure 13.

The simulation results showed that, after the use of novel rail dampers, the difference in wheel-track receptance difference above f_0 decreased. Furthermore, the comparison of the difference in wheel-track receptance at the first vertical and lateral pinned-pinned frequency for rail with and without dampers is shown in Figure 14. It can be found that, after the use of novel rail dampers, the difference in the maximum vertical wheel-track receptance decreased from 41.5 dB to 32.5 dB at midspan, and the difference in the maximum vertical minimum wheel-track receptance decreased from 16.5 dB to 8.5 dB on support. The average reduction of the

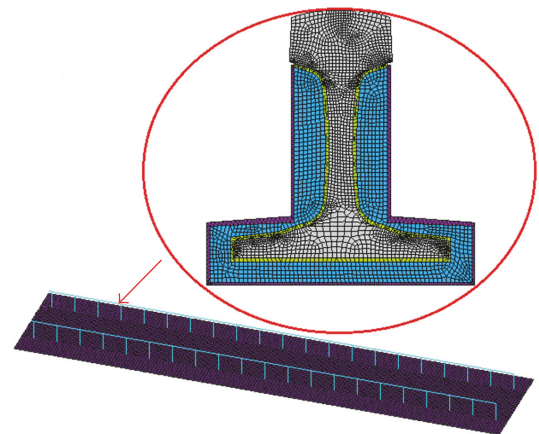


FIGURE 12: Overview of the finite element model and close-ups of the rail with slotted stand-off layer damper.

difference in wheel-track receptance along the longitudinal direction of the rail reached 8.7 dB, which means that the vertical impact effect between the rail and wheel can be effectively reduced by the novel dampers.

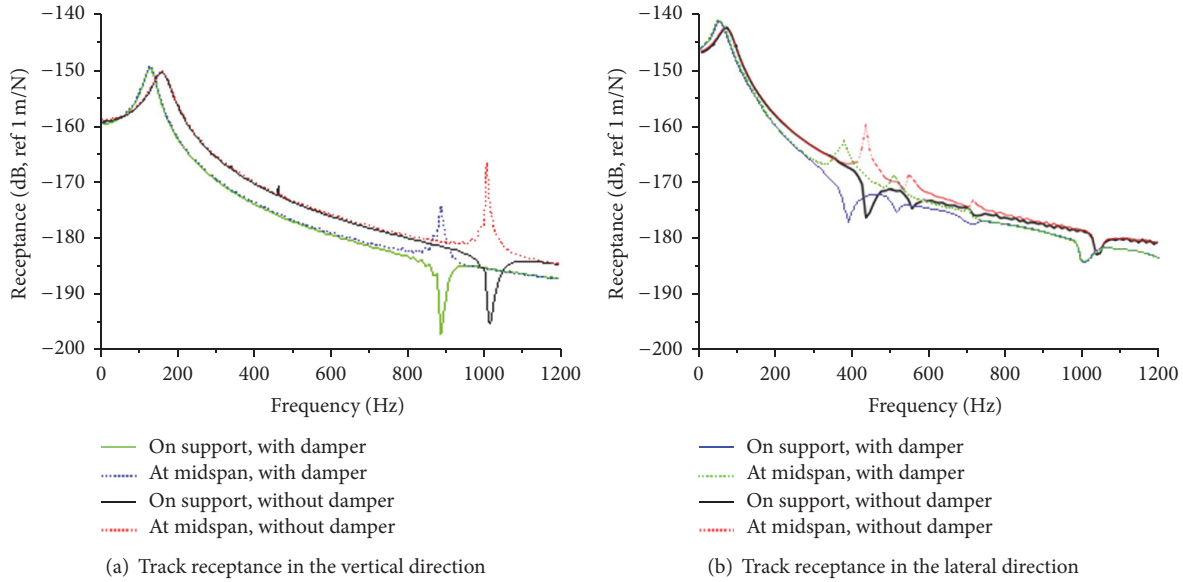


FIGURE 13: Receptance spectra of the track with dampers.

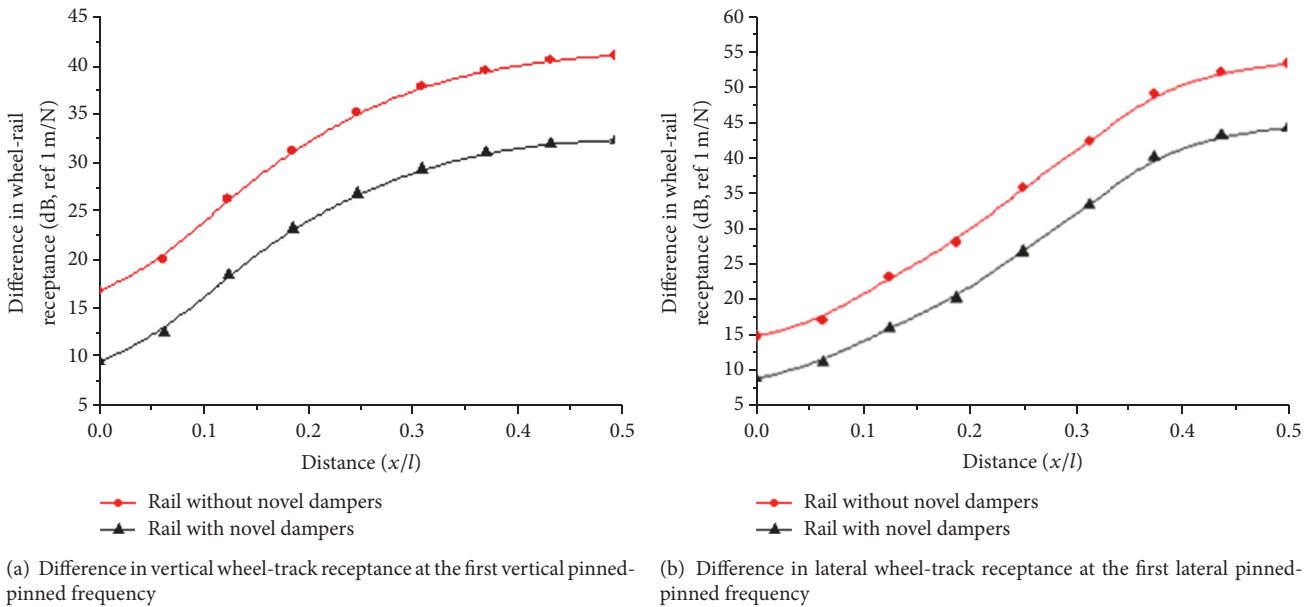


FIGURE 14: Effect of rail dampers on suppressing the difference in wheel-track receptance.

Figure 14(b) shows that the lateral maximum wheel-track receptance difference decreased from 53 dB to 44 dB at midspan after the application of the novel dampers. The lateral minimum value decreased from 15 dB to 9 dB after the application of the novel dampers. The reduction in the receptance difference was significant, with an average reduction of 7.6 dB. Therefore, the use of the novel rail dampers is an effective tool to control the lateral sliding wheel-rail wearing effects. In theory, the novel rail dampers could minimize the short-pitch rail corrugation that appeared in Chongqing metro line 2.

After the adoption of the novel rail dampers, the difference in vertical and lateral wheel-track receptance decreased sharply for two main reasons. The novel rail dampers shifted the pinned-pinned frequency from a higher frequency range to a lower frequency range, with the first vertical pinned-pinned frequency shifting from 1020 Hz to 882 Hz and the lateral pinned-pinned frequency shifting from 440 Hz to 396 Hz. Based on the wheel and track receptance spectra, the wheel-track receptance difference at the pinned-pinned frequency decreased when the pinned-pinned frequency moved towards the lower frequency. The novel rail dampers

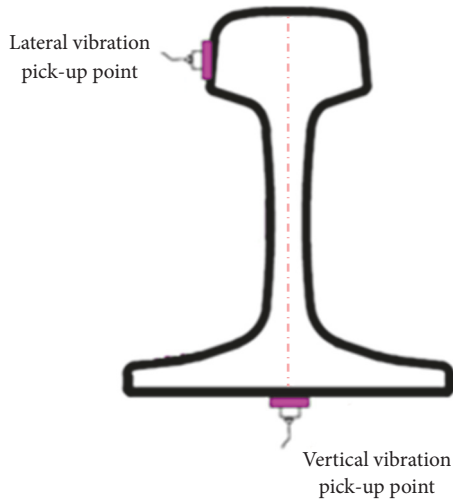


FIGURE 15: Location of the vibration pick-up points.

smoothed the track receptance and transformed the vibration energy of the rail into heat, lowering the rail vibration response, especially at the pinned-pinned frequency.

5. Experimental Verification of the Short-Pitch Rail Corrugation Growth

5.1. Test Methods and Setup. For a better comparison with in situ measured results, rail grinding was used to eliminate the short-pitch rail corrugation before the installation of the novel rail dampers. To evaluate and verify the practical suppression effect of rail dampers on short-pitch rail corrugation, tests without and with the novel rail dampers were conducted. Furthermore, the content of the present measurements was divided into two different stages that focused on the evaluation of the control effect of the novel rail dampers on the vibration performance of rails and on short-pitch rail corrugation initiation and growth when a metro train passes through this section at the required speed.

A rail vibration test was performed to evaluate the control effect of the settlement on the wheel-rail interaction mentioned in this research. Two accelerometers were placed at two locations: at the rail head side and at the bottom of the rail, as shown in Figure 15. The short-pitch rail corrugation was investigated via in situ observation.

5.2. Vibration Response of the Rails. The vibration acceleration level in each one-third octave band at the two major parts of the rail with and without dampers is illustrated in Figure 16. Figures 16(a) and 16(b) show that, after the adoption of the novel rail dampers, the lateral vibration of the rail was significantly reduced. In addition, the vibration fell heavily below 100 Hz. This reduction is mainly due to the increase of the overall rail mass. The mass of Chinese 60 kg/m rail per metre is 60 kg, and the mass of the rail damper per metre is 15 kg. Therefore, after the installation of the damper, the mass of the rail per metre increased from 60 kg to 75 kg.

The increase of the rail mass attenuated the vibration level of the rail at low frequency. Another significant reduction is at approximately 400 Hz, with a reduction of 11 dB. Generally, there are two reasons for this reduction. The first is that the viscoelastic damping layer inside the rail damper transformed the vibration energy into heat and resulted in the reduction of rail vibration. The second and most important reason is that the application of the rail dampers shifts the first pinned-pinned frequency from 440 Hz to 396 Hz and decreases the wheel-track receptance difference at the first pinned-pinned frequency, ultimately minimizing the wheel-track force.

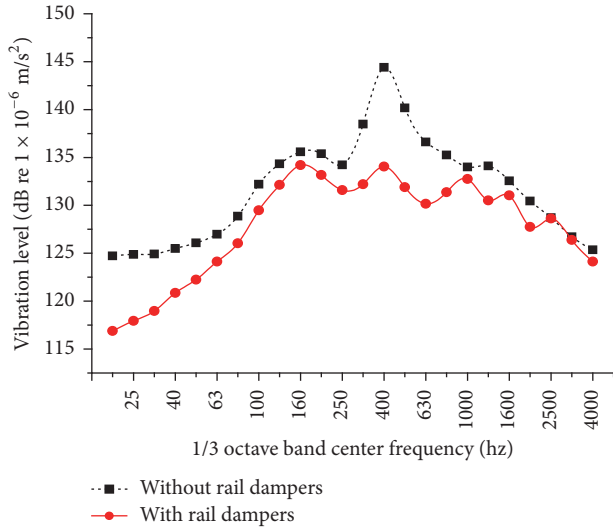
Figures 16(c) and 16(d) represent the vertical acceleration vibration level of the rail bottom. The use of rail dampers also decreased the vertical vibration levels of the rail foot below 4000 Hz. The reason is the same as that mentioned for the lateral vibration. The implementation of rail dampers reduced the lateral and vertical vibration of the rail. This means that the rail damper could effectively minimize the wheel-rail interaction, wheel-rail force, and wheel-rail vibration.

5.3. In Situ Observation of Short-Pitch Rail Corrugation Initiation and Growth. The second in situ observation was at the same site as the first observation in Chongqing metro line 2. It was a double track metro line. There was short-pitch rail corrugation in both lines following a period of time after the opening of the railway line, as shown in Figure 17(a). To more precisely evaluate the suppression effect of the novel rail dampers on short-pitch rail corrugation initiation and growth, before the application of the novel rail dampers, rail grinding was used to remove the short-pitch rail corrugation on both lines. The novel rail dampers were installed on only one of the lines, as shown in Figure 17(b).

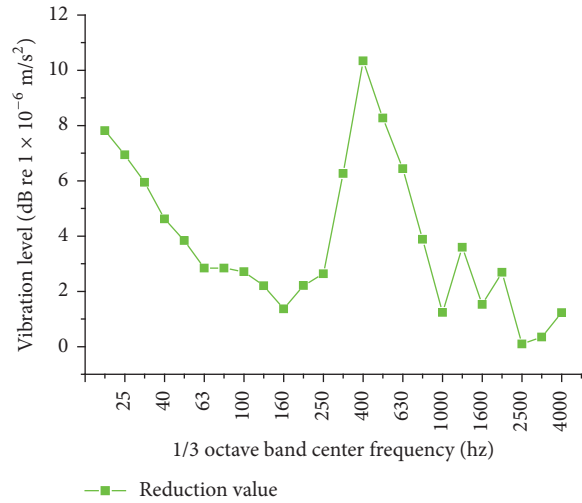
Six months later, there was a significant difference between the line with the novel rail dampers and the line without them. As shown in Figure 17(c), apparent short-pitch rail corrugation reappeared on the line without the novel rail dampers because the rail grinding only removed the original short-pitch rail corrugation and could not change the dynamic properties of the track or abate the difference in wheel-track receptance. Figure 17(d) shows that there was no visible short-pitch rail corrugation on the line with the novel rail dampers. Comparing Figure 17(c) with 17(d) proved that the novel rail dampers could effectively minimize short-pitch rail corrugation at the Chongqing metro line 2.

6. Conclusions

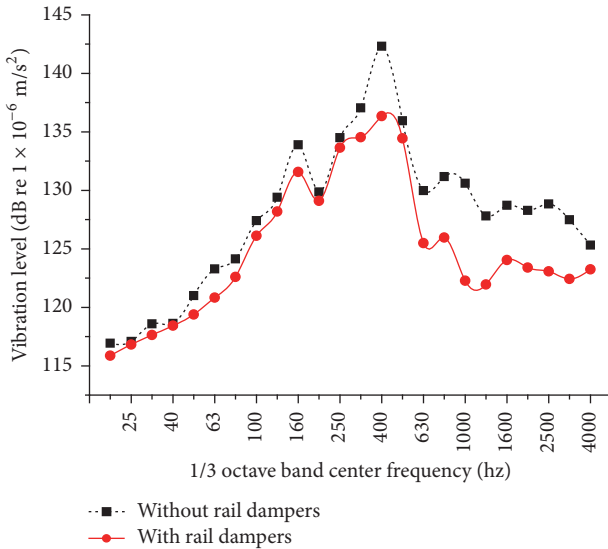
The aim of this work was to study the ability of rail dampers to minimize the short-pitch rail corrugation that appeared on Chongqing metro line 2. The configuration and mechanism of initiation of short-pitch rail corrugation were investigated by theoretical simulation and experimental validation. The likelihood of the occurrence of this short-pitch rail corrugation on the track with Cologne-egg fastening system was minimized by applying rail dampers. The following conclusions can be drawn based on these field experimental and theoretical studies.



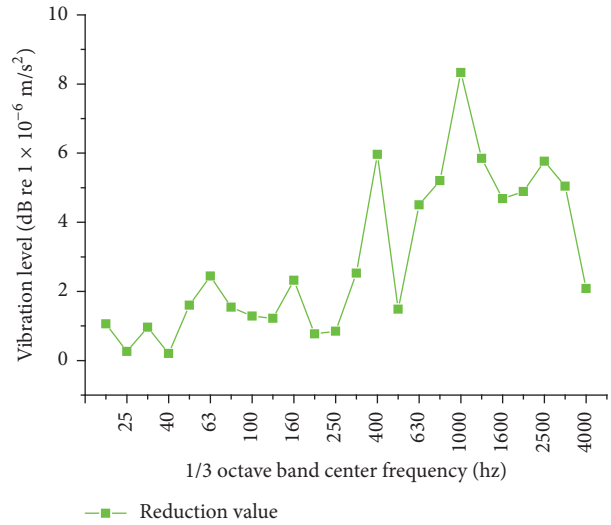
(a) Lateral acceleration vibration level of the rail head side



(b) Reduction value of the lateral acceleration vibration level



(c) Vertical acceleration vibration level of the rail bottom



(d) Reduction value of the vertical acceleration vibration level

FIGURE 16: Acceleration of the rail with and without dampers.

- (1) Wheel-rail resonance occurs at 440 Hz on the tracks with Cologne-egg fastening system in Chongqing metro line 2, and it is the main cause of vibration and short-pitch rail corrugation. The vibration mode of the track at this short-pitch rail corrugation frequency was generated using a first-order lateral pinned-pinned resonance. The fixed moving speed of the wheel and the large difference in wheel-track receptance at the first lateral pinned-pinned frequency are the main reasons for the short-pitch rail corrugation.
- (2) The installation of novel rail dampers could sharply decrease the lateral and vertical wheel-track receptance at the first lateral pinned-pinned frequency. This reduction occurs for two main reasons. On the one hand, the novel rail dampers shifted the pinned-pinned frequency from a higher frequency range to a

lower frequency range, with the first vertical pinned-pinned frequency shifting from 1020 Hz to 882 Hz and the lateral pinned-pinned frequency shifting from 440 Hz to 396 Hz. On the other hand, the novel rail dampers smoothed the track receptance and transformed the vibration energy of the rail into heat, reducing the difference in wheel-track receptance, especially at the first lateral pinned-pinned frequency.

- (3) The in situ verification experiment showed that the implementation of rail dampers could reduce the lateral and vertical vibration of the rail. It means rail damper could effectively minimize wheel-rail interaction, wheel-rail force, and wheel-rail vibration. And the in situ observation of short-pitch rail corrugation depicted that, after six months, the short-pitch rail corrugation appeared again on the track without rail

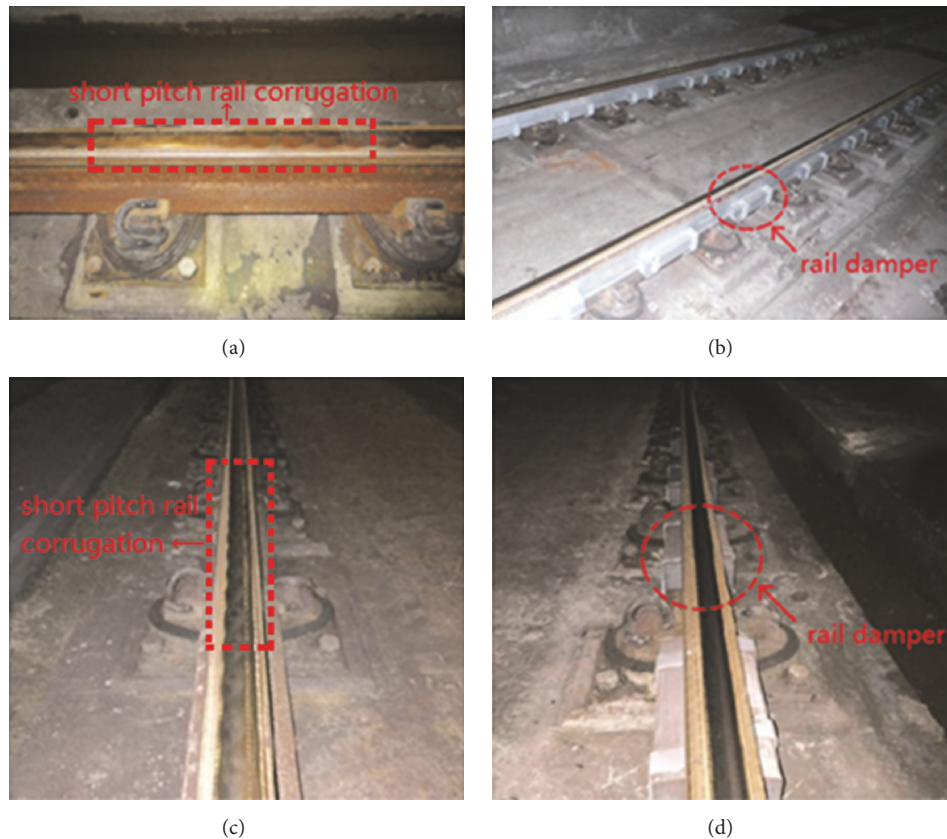


FIGURE 17: Second in situ observation of short-pitch rail corrugation at the Chongqing metro line 2. (a) Original short-pitch rail corrugation that appeared in both lines. (b) Rail dampers were installed on one line after rail grinding. (c) Short-pitch rail corrugation reappeared on the line without rail dampers. (d) Minimal short-pitch rail corrugation reappeared on the line with rail dampers.

dampers and there was no visible short-pitch rail corrugation on the track with rail dampers. It proved that the novel rail dampers can effectively minimize the short-pitch rail corrugation on Chongqing metro line 2.

Conflicts of Interest

The authors declare that there are no conflicts of interest regarding the publication of this paper. The mentioned received funding in the “Acknowledgments” did not lead to any conflicts of interest regarding the publication of this manuscript. There are no other possible conflicts of interest in the manuscript.

Acknowledgments

Thanks are owed to the NSFC (National Natural Science Foundation of China, no. U1234201 and no. U1334203) for the research grants awarded to the corresponding author. The work described in this paper was supported by the National Natural Science Foundation of China (51508479) and the Research Fund for the Doctoral Program of Higher Education of China (2682015CX079).

References

- [1] C. Talotte, P.-E. Gautier, D. J. Thompson, and C. Hanson, “Identification, modelling and reduction potential of railway noise sources: a critical survey,” *Journal of Sound and Vibration*, vol. 267, no. 3, pp. 447–468, 2003.
- [2] Z. Yan, V. Markine, A. Gu, and Q. Liang, “Optimisation of the dynamic properties of ladder track to minimise the chance of rail corrugation,” *Proceedings of the Institution of Mechanical Engineers, Part F: Journal of Rail and Rapid Transit*, vol. 228, no. 3, pp. 285–297, 2014.
- [3] S. L. Grassie and J. Kalousek, “Rail corrugation: characteristics, causes and treatments,” *Proceedings of the Institution of Mechanical Engineers, Part F: Journal of Rail and Rapid Transit*, vol. 207, no. 1, pp. 57–68, 1993.
- [4] K. H. Oostermeijer, “Review on short pitch rail corrugation studies,” *Wear*, vol. 265, no. 9-10, pp. 1231–1237, 2008.
- [5] C. O. Frederick and W. G. Bugden, “Corrugation research on British Rail,” in *Proceedings of the Symposium on Rail Corrugation Problems*, K. Knothe and R. Gasch, Eds., pp. 7–33, Technische Universität Berlin, Berlin, Germany, July 1983.
- [6] C. O. Frederick, “A rail corrugation theory,” in *Proceedings of the 2nd Conference on the Contact Mechanics and Wear of Rail/Wheel Systems*, pp. 268–275, Vancouver, Canada, 1986.
- [7] Y. Sato, A. Matsumoto, and K. Knothe, “Review on rail corrugation studies,” *Wear*, vol. 253, no. 1-2, pp. 130–139, 2002.

- [8] S. L. Grassie, "Rail corrugation: characteristics, causes, and treatments," *Proceedings of the Institution of Mechanical Engineers, Part F: Journal of Rail and Rapid Transit*, vol. 223, no. 6, pp. 581–596, 2009.
- [9] Z. Yan, A. Gu, W. Liu, V. L. Markine, and Q. Liang, "Effects of wheelset vibration on initiation and evolution of rail short-pitch corrugation," *Journal of Central South University*, vol. 19, no. 9, pp. 2681–2688, 2012.
- [10] X. Li, W. Li, H. Y. Wang et al., "Study on the mechanism of rail corrugation of subway track with vibration-absorbing fasteners," in *Proceedings of the 9th International Conference on Contact Mechanics and Wear of Rail/Wheel Systems*, pp. 205–215, Chengdu, China, 2012.
- [11] A. Wang, Z. Wang, P. Zhang et al., "Study on the mechanism of discontinuous support stiffness on the development of rail corrugation," in *Proceedings of the 21st International Congress on Sound and Vibration*, pp. 13–17, Beijing, China, 2014.
- [12] S. L. Grassie and J. A. Elkins, "Rail corrugation on North American transit systems," *Vehicle System Dynamics*, vol. 29, pp. 5–17, 1998.
- [13] O. Oyarzabal, J. Gómez, J. Santamaría, and E. G. Vadillo, "Dynamic optimization of track components to minimize rail corrugation," *Journal of Sound and Vibration*, vol. 319, no. 3–5, pp. 904–917, 2009.
- [14] J. I. Egana, J. Vinolas, and M. Seco, "Investigation of the influence of rail pad stiffness on rail corrugation on a transit system," *Wear*, vol. 261, no. 2, pp. 216–224, 2006.
- [15] E. G. Vadillo, J. A. Tárrago, G. G. Zubiaurre, and C. A. Duque, "Effect of sleeper distance on rail corrugation," *Wear*, vol. 217, no. 1, pp. 140–146, 1998.
- [16] H. Chen, S. Fukagai, Y. Sone, T. Ban, and A. Namura, "Assessment of lubricant applied to wheel/rail interface in curves," *Wear*, vol. 314, no. 1-2, pp. 228–235, 2014.
- [17] B. E. Croft, C. J. C. Jones, and D. J. Thompson, "Modelling the effect of rail dampers on wheel-rail interaction forces and rail roughness growth rates," *Journal of Sound and Vibration*, vol. 323, no. 1-2, pp. 17–32, 2009.
- [18] T. X. Wu, "Effects on short pitch rail corrugation growth of a rail vibration absorber/damper," *Wear*, vol. 271, no. 1-2, pp. 339–348, 2011.
- [19] A. P. De Man, "Pin-pin resonance as a reference in determining ballasted railway track vibration behaviour," *Heron*, vol. 45, no. 1, pp. 35–51, 2000.
- [20] C. Zhao and P. Wang, "Theoretical modelling and effectiveness study of slotted stand-off layer damping treatment for rail vibration and noise control," *Shock and Vibration*, vol. 2015, Article ID 716382, 12 pages, 2015.
- [21] R. Gustavson and K. Gylltoft, "Influence of cracked sleepers on the global track response: coupling of a linear track model and non-linear finite element analyses," *Proceedings of the Institution of Mechanical Engineers Part F: Journal of Rail and Rapid Transit*, vol. 216, no. 1, pp. 41–51, 2002.



Hindawi

Submit your manuscripts at
<https://www.hindawi.com>

